RSC Advances

ROYAL SOCIETY OF CHEMISTRY

www.rsc.org/advances

Journal Name

ARTICLE

Efficient perovskite solar cell fabricated in ambient air using one-step spin-coating

Received 00th January 20xx,
Accepted 00th January 20xx

DOI: 10.1039/x0xx00000x
www.rsc.org/

Gang Wang[a,b], Debei Liu[a,b], Jin Xiang[a,b], Dachen Zhou[a,b], Kamal Alameh[c], Baofu Ding[a,c] and Qunliang Song[a,b,c*]

One-step spin coating is a simple method which has been widely used in fabricating perovskite solar cells. However, this method was vastly demonstrated in glove box wherein the influence of moisture is negligible. Thus the use of one-step spin-coating in ambient air has not been comprehensively investigated. In this work, we employ one-step spin-coating method to coat perovskite films in ambient air (with humidity above 50%), and then the perovskite films are annealed in vaccum or air. Experimental results show that by using vacuum annealing, a power conversion efficiency of 12.98% is attained, and this is 45% higher than that attained by air annealing method. This improvement is mainly attributed to the fast solvent evaporation process in vacuum during annealing, which induces high supersaturation that leads to higher coverage of perovskite films.

1. Introduction

Organic-inorganic metal halide perovskite compounds have attracted a significant amount of attention[1-4], due to their strong light absorption, long charge carrier lifetime and diffusion length. Over the last six years, the power conversion efficiency (PCE) of organic-inorganic perovskite solar cells had increased from 3.8%[5] to 20.8%[6]. This dramatical improvement in performance is mainly attributed to the efforts devoted towards the precise control of their fabrication processes and conditions. In particular, the mitigation of the influence of moisture has been intensively investigated for various perovskite compound fabrication methods, including vacuum vapor-deposition[7, 8], solution processing in glove box (including one-step spin-coating[9, 10], two-step spin-coating[11] and two-step sequential deposition[12]). However, these fabrication methods are still cost-ineffective for the mass-production of large-scale perovskite solar cells. Recently, several special methods for fabricating high-efficiency perovskite solar cells in ambient air have been reported[13]. Hyun-Seok Ko et al.[14] have demonstrated a PCE of 15.8% for perovskite solar cells fabricated using two-step spin-coating under 50% relative humidity. Paifeng Luo et al.[15] have fabricated perovskite solar cells using low-pressure chemical vapour deposition under open-air with humidity above 60%, attaining a PCE of 12.73%. Zhurong Liang et al.[16] have prepared perovskite solar cells under a relative humidity of 50% using spray deposition, achieving a PCE around 7.9%.

One-step spin-coating methods have been proposed and intensively investigated[17-21]. You et al.[22]firstly reported that proper moisture can assist $CH_3NH_3PbI_3$ ($MAPbI_3$) perovskite-film growth during annealing, and hence improving the performance of solar cells. Another similar study has demonstrated that annealing $MAPbI_3$ perovskite films in ambient air leads to better performance in comparison with films annealed in dry air[23, 24]. Gao et al.[25] argued that though moisture has a positive effect on the perovskite crystal growth at the annealing stage, it has a negative effect on the nucleation at the spin-coating stage, thus leading to less film coverage. Sang Hyuk Im introduced moisture in the spin-coating stage by adding aqueous HI in perovskite precursor solution, and achieved a high efficiency through fast annealing in air[26, 27]. These one-step spin-coating methods have demonstrated that the common issue of low perovskite film coverage at spin-coating stage can be overcome through careful control of the moisture during annealing. By carefully controlling spin-coating and annealing conditions, a high-quality high-efficiency perovskite solar cells can be developed.

Besides annealing in air, a method based on annealing in vacuum has been proposed for effective perovskite crystal growth. However, for this method, exposure to air or other solvent vapours have been avoided in order to achieve better performance[28]. In this work, we fabricate perovskite solar cells using one-step spin-coating in ambient air (with a relative humidity above 50%). By vacuum annealing the perovskite films (coated in ambient air), high coverage of perovskite films have been achieved. Experimental results show that, the perovskite solar cell annealed in vacuum exhibited a PCE as high as 12.98%.

[a] Institute for Clean Energy and Advanced Materials, Faculty of Materials and Energy, Southwest University, Chongqing 400715, P. R. China
[b] Chongqing Key Laboratory for Advanced Materials and Technologies of Clean Energy, Chongqing 400715, P. R. China
[c] Electron Science Research Institute, Edith Cowan University, 270 Joondalup Drive, Joondalup, WA, 6027 Australia

†Electronic Supplementary Information (ESI) available: Annealing process for the devices. Example of J–V curves displaying hysteresis. Compositional data of EDS and XPS. See DOI: 10.1039/x0xx00000x

2. Experiment

Materials: $PbCl_2$, methyl ammonium iodide (MAI), phenyl-C61-butyric acid methyl ester (PCBM), Poly(3,4-ethylenedioxythiophene)poly(styrenesulfonate)(PEDOT:PSS) were all purchased from Xi'an Polymer Light Technology Corp (China), while N,N-dimethylformide (DMF) and chlorobenzene were from Sigma–Aldrich. The perovskite precursor solution was prepared using the method reported in Ref. 29. MAI and $PbCl_2$ were dissolved in DMF at 3:1 molar ratio with a concentration of 2.4 M MAI and 0.8 M $PbCl_2$ and stirred overnight under room temperature. 20 mg PCBM was dissolved in 1 ml chlorobenzene and stirred overnight under room temperature.

Solar cell fabrication: The Indium-Tin Oxide (ITO) substrate was cleaned with a mild detergent, rinsed several times with distilled water and subsequently with ethanol in an ultrasonic bath, finally dried under nitrogen stream. Then a single layer of PEDOT:PSS was spin-coated on ITO at 6000 rpm for 60 s and subsequently annealed at 120℃ for 20 min. The perovskite precursor solution was filtered with a PTFE syringe filter (Whatman, 0.45 μm) and spin-coated on PEDOT:PSS at 2000 rpm for 60 s. Then the film was heated to 95℃ for 90 min in a vacuum oven (~200 mbar) to form and crystallize the perovskite film. The reference devices were fabricated in the same way, the only difference is that annealing was conducted on a hot plate in air. The PCBM layer was then deposited onto the perovskite film from a chlorobenzene solution (20 mg/mL) using spin-coating in air with a speed of 6000 rpm for 40 s. Finally, 20 nm C60 and 120 nm aluminum (Al) electrodes were sequentially deposited in high vacuum using a shadow mask. The cell area, defined as the crossing area between the ITO and Al electrode, was 0.09 cm^2. All spin-coating processes were completed in ambient air with relative humidity of 50±5%

Characterization: The crystal structures of the perovskite films were characterized using an X-ray diffraction system (Shimadzu XRD-7000). The morphologies of the developed structures were examined using field-emission scanning electron microscopy (SEM, JSM-6700F). UV-Vis absorption measurements were carried out using Shimadzu UV-2550 spectrometer. The J-V characteristics of the developed devices were mesured using Keithley 2400 in conjunction with Newport 94043A solar simulator, which generated 100 mW/cm^2 (AM 1.5 G) simulated sunlight. The J-V curves were measured in reverse (from 1.2 V to -1.2 V) or forward (from -1.2 V to 1.2 V) scan (with a voltage step of 10 mV and 0 ms delay time). The external quantum efficiency (EQE) of the devices was calculated from the photocurrent measured using a lock-in amplifier (SR-830). After fabrication, the J-V and EQE characteristics were measured in the glove box.

3. Results and discussion

3.1 XRD and SEM characterization

The XRD patterns of the perovskite films, annealed in air and vacuum, are shown in Fig. 1. The main diffraction peaks of perovskite are found at 14.14°, 28.48°, 31.92°, which can be assigned to the (110), (220), (310), orthorhombic crystal structure peaks for $MAPbI_3$[30]. Though $PbCl_2$ was used, none of the $NH_3CH_3PbCl_3$ diffraction peaks was observed, because most of the chloride ions escaped with NH_3CH_3Cl during annealing in air or vacuum[23, 28]. The residual chloride was analysed using an energy-dispersive X-ray system (EDS) and X-ray photoelectron spectroscopy (XPS) system (see supporting information Fig.S3 and Fig.S4). Results showed that the amount of residual chloride in perovskite films annealed in vacuum is higher than that in films annealed in air. Furthermore, the intensities of the

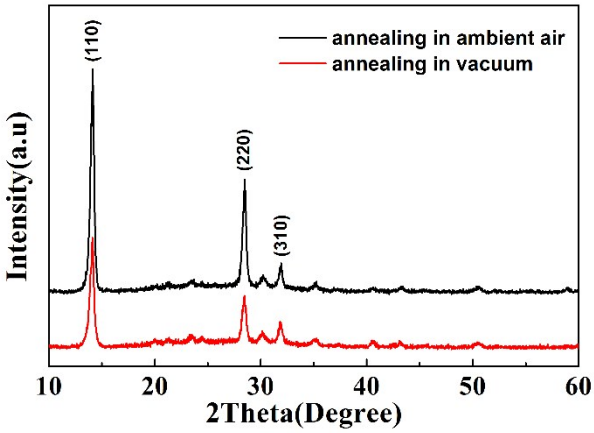

Figure 1. XRD patterns of perovskite films annealed with different methods.

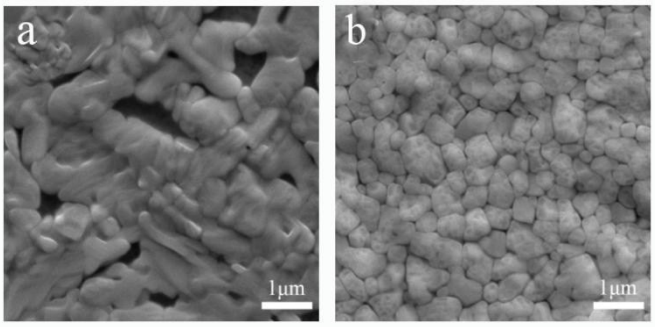

Figure 2. SEM images of perovskite films annealed in ambient air (a) and in vacuum (b).

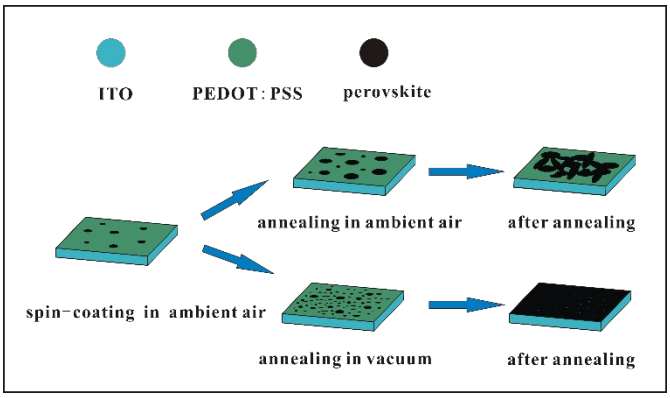

Figure 3. The processes of crystal growth for different annealing methods.

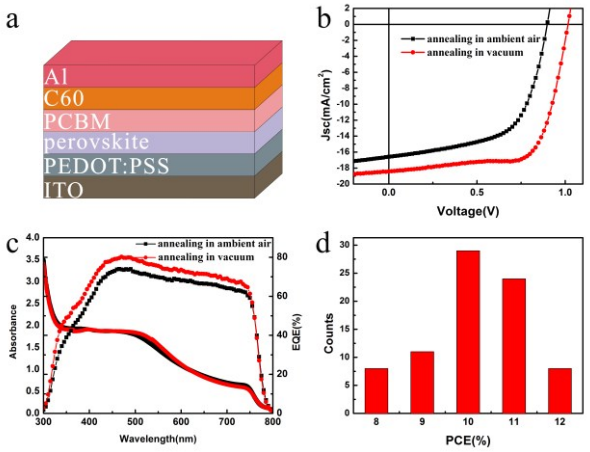

Figure 4. (a) The device structure is ITO/PEDOT:PSS/$CH_3NH_3PbI_{3-x}Cl_x$/PCBM/C60/Al. (b) J-V curve of the devices with the perovskite films annealed in different methods(reverse scan). (c) EQE and absorbance of the corresponding devices. (d)The PCE histogram for 80 devices annealed in vacuum.

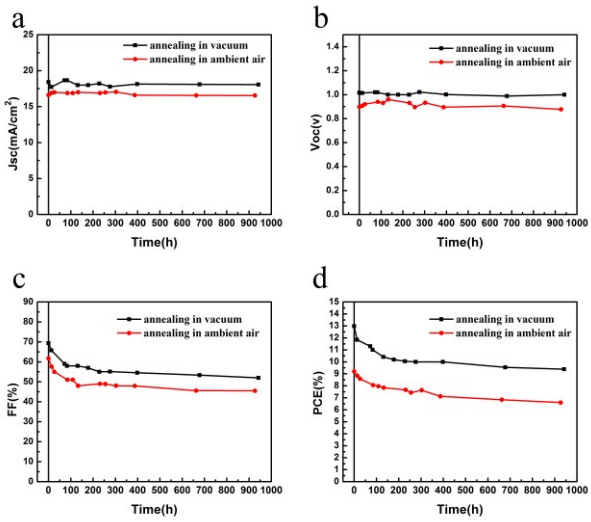

Figure 5. Long-term stability test of the perovskite solar cells in glove box.

diffraction peaks of (110) and (220) of devices annealed in ambient air are stronger than that of devices annealed in vacuum. This means the enhanced crystallinity of perovskite films were formed under ambient conditions[16]. This is due to the moisture assisted perovskite film growth during annealing in air[22].

SEM images of the perovskite films, annealed in air and vacuum, are compared in Figs. 2 (a and b), which show that the films annealed in air exhibit a larger grain size (1-1.5 µm) with irregular large gaps (Fig. 2a), while perovskite films annealed in vacuum exhibit relatively smoother surfaces with fewer gaps (Fig. 2b). It has been suggested that, a fast nucleation at the spin-coating stage followed by modest crystal growth at the annealing stage, can result in the formation of high-quality perovskite films[25]. Spin-coating in humid air, the moisture will decrease the supersaturation of perovskite solution, leading to large critical nucleus radius, low nucleation density, and island growth of perovskite film[25]. Typically, with annealing in air new nucleations are hardly formed, due to the relatively high moisture. Therefore, the moisture will enhance island growth during annealing, leading to large crystals with rough surfaces, as shown in Fig. 2a. For annealing in vacuum, the fast evaporation of solvent increases the supersaturation in the residual solvent between the island crystals. Those newly nucleated perovskite crystals (due to supersaturation under vacuum condition) connect the adjacent grains formed during spin-coating, resulting in smaller gaps between grains and higher perovskite film coverage as evidenced from Fig. 2b[25, 31]. The processes of crystal growth when annealing in air and vacuum are schematically displayed in Fig. 3.

3.2 Photovoltaic performance of champion cell

We fabricated devices with the structure of ITO/PEDOT:PSS/$CH_3NH_3PbI_{3-x}Cl_x$/PCBM/C_{60}/Al, shown in Fig. 4a. The J-V characteristics of the devices for different annealing methods are shown in Fig. 4b. The reference device, whose perovskite film was annealed in air, shows a PCE of approximate 9.2%. The measured short circuit current density (J_{sc}), open circuit voltage (V_{oc}), and fill factor (FF) were 16.59 mA/cm^2, 0.89 V, and 61.8%, respectively. By annealing the perovskite film in vacuum, the PCE increased to 12.98%, while the measured J_{sc}, V_{oc}, and FF values were 18.42 mA/cm^2, 1.02 V and 69.4 %, respectively. The EQE and absorbance of the developed devices are displayed, for comparison, in Fig. 4c, showing that the EQE of the device annealed in vacuum is higher than that annealed in ambient air. The integrated current densities of devices annealed in vacuum and in air are 17.87 mA/cm^2 and 16.31 mA/cm^2, respectively, which are consistent with the J-V measurements. Note that, although the annealing methods are different, the light absorbance of the films are similar, as shown in the UV-Vis measurements shown in Fig. 4c. Thus the larger J_{sc} of the device annealed in vacuum can be attributed to the better connectivity between perovskite grains and/or the connectivity between the perovskite film and the electrodes, as evidenced from the SEM images displayed in Fig. 2. Note also that, the higher FF and V_{oc} of the device annealed in vacuum can be inferred from the better coverage of the perovskite film annealed in vacuum. The positive correlation between the device performance and the coverage of perovskite film has been reported elsewhere[32]. Another contribution to the performance improvement achieved by using vacuum annealing method might be the residual chloride in the film, which enhances the diffusion length of the carrier[1]. It is important to note that the perovskite solar cells exhibit J-V hysteresis with the scan direction. For the device annealed in vacuum, the highest PCE of 12.98% was achieved with a reverse scan. However, the PCE dropped to 10.49% with a forward scan. A similar hysteresis behaviour was also observed for the device annealed in air. The J-V hysteresis curves are presented in the Supporting Information, Fig. S2. The reproducibility of our method was checked by characterizing a batch of 80 devices. For more than 73% of the devices annealed in vacuum, the PCE

was higher than 10%, and the average efficiency for all eighty devices was 10.65%. The PCE histograms of these 80 devices are displayed in Fig. 4d. On the other hand, the average efficiency for the devices annealed in air was 7.63%.

3.3 The stability of devices

To further illustrate the effect of the annealing processes on the durability of the perovskite film after spin coating in air, the stability of devices were tested. All cells were tested in a high-purity N_2 filled glove box after fabrication. As shown in Fig. 5a and 5b, the J_{sc} and V_{oc} of the devices were very stable in the glove box over 1000 hours, for both perovskite films annealed in air and in vacuum. The degradation of the PCE displayed in Fig. 5d is mainly due to the decrease of FF, especially the fast decrease in the initial 150 h (about 20% decrease during this duration), as shown in Fig. 5c and 5d. Unfortunately, all the perovskite solar cells, either annealed in air or in vacuum, exhibited very short lifetime when testing in ambient air.

4. Conclusion

By introducing the vacuum annealing, we have fabricated perovskite solar cells with improved performance from one-step spin-coating in ambient air with humidity of 50±5%. An efficiency of 12.98% in $CH_3NH_3PbI_{3-x}Cl_x$ solar cell has been attained using this method with good stability in pure N2 environment. Compared with annealing in air, the improved device performance is mainly attributed to the high surface coverage of the perovskite films developed through vacuum annealing. The one-step spin-coating in air followed by vacuum annealing is a cost-effective method that can realise high-efficiency perovskite solar cells without the need for high-cost development in a glove box.

5. Acknowledgments

This work was supported by the National Natural Science Foundation of China (Grant No. 11274256) and the Fundamental Research Funds for the Central Universities (XDJK2014A006). This work was also partially sponsored by Doctoral Fund of Ministry of Education of China (20120182110008).

References

1. S. D. Stranks, G. E. Eperon, G. Grancini, C. Menelaou, M. J. P. Alcocer, T. Leijtens, L. M. Herz, A. Petrozza and H. J. Snaith, *Science*, 2013, **342**, 341-344.
2. G. Xing, N. Mathews, S. Sun, S. S. Lim, Y. M. Lam, M. Graetzel, S. Mhaisalkar and T. C. Sum, *Science*, 2013, **342**, 344-347.
3. C. Wehrenfennig, G. E. Eperon, M. B. Johnston, H. J. Snaith and L. M. Herz, *Adv. Mater.*, 2014, **26**, 1584-1589.
4. S. Gamliel and L. Etgar, *RSC Adv*, 2014, **4**, 29012-29021.
5. A. Kojima, K. Teshima, Y. Shirai and T. Miyasaka, *J. Am. Chem.* Soc., 2009, 131, 6050-6051.
6. D. Bi, W. Tress, M. I. Dar, P. Gao, J. Luo, C. Renevier, K. Schenk, A. Abate, F. Giordano, J. P. Correa Baena, J. D. Decoppet, S. M. Zakeeruddin, M. K. Nazeeruddin, M. Gratzel and A. Hagfeldt, Science advances, 2016, **2**, e1501170..
7. M. Liu, M. B. Johnston and H. J. Snaith, Nature, 2013, 501, 395-398.
8. H. Hu, D. Wang, Y. Zhou, J. Zhang, S. Lv, S. Pang, X. Chen, Z. Liu, N. P. Padture and G. Cui, RSC Adv, 2014, 4, 28964-28967.
9. H. S. Kim, C. R. Lee, J. H. Im, K. B. Lee, T. Moehl, A. Marchioro, S. J. Moon, R. Humphry-Baker, J. H. Yum, J. E. Moser, M. Gratzel and N. G. Park, *Sci. Rep.*, 2012, **2**, 591.
10. M. M. Lee, J. Teuscher, T. Miyasaka, T. N. Murakami and H. J. Snaith, *Science*, 2012, **338**, 643-647.
11. Z. Xiao, C. Bi, Y. Shao, Q. Dong, Q. Wang, Y. Yuan, C. Wang, Y. Gao and J. Huang, *Energy Enviro. Sci.*, 2014,7,2619-262312. J. Burschka, N. Pellet, S. J. Moon, R. Humphry-Baker, P. Gao, M. K. Nazeeruddin and M. Gratzel, *Nature*, 2013, **499**, 316-319.
13. Y. Du, H. Cai, J. Ni, J. Li, H. Yu, X. Sun, Y. Wu, H. Wen and J. Zhang, *RSC Adv.*, 2015, **5**, 66981-66987.
14. H.-S. Ko, J.-W. Lee and N.-G. Park, *J. Mater. Chem. A*, 2015, **3**, 8808-8815.
15. P. Luo, Z. Liu, W. Xia, C. Yuan, J. Cheng and Y. Lu, ACS Appl. Mater. Interfaces, 2015, 7, 2708-2714.
16. Z. Liang, S. Zhang, X. Xu, N. Wang, J. Wang, X. Wang, Z. Bi, G. Xu, N. Yuan and J. Ding, *RSC Adv*, 2015, **5**, 60562-60569.
17. P. Docampo, J. M. Ball, M. Darwich, G. E. Eperon and H. J. Snaith, *Nat. commun.*, 2013, **4**, 2761.
18. J. H. Heo, S. H. Im, J. H. Noh, T. N. Mandal, C.-S. Lim, J. A. Chang, Y. H. Lee, H.-j. Kim, A. Sarkar, M. K. Nazeeruddin, M. Grätzel and S. I. Seok, *Nat. Photonics*, 2013, **7**, 486-491.
19. H. Zhou, Q. Chen, G. Li, S. Luo, T.-b. Song, H.-S. Duan, Z. Hong, J. You, Y. Liu and Y. Yang, *Science*, 2014, **345**, 542-546.
20. J. M. Ball, M. M. Lee, A. Hey and H. J. Snaith, *Energy Enviro. Sci.*, 2013, **6**, 1739-1743.
21. J. Y. Jeng, Y. F. Chiang, M. H. Lee, S. R. Peng, T. F. Guo, P. Chen and T. C. Wen, *Adv. Mater.*, 2013, **25**, 3727-3732.
22. J. You, Y. Yang, Z. Hong, T.-B. Song, L. Meng, Y. Liu, C. Jiang, H. Zhou, W.-H. Chang, G. Li and Y. Yang, *Appl. Phys. Lett.*, 2014, **105**, 183902.
23. S. R. Raga, M.-C. Jung, M. V. Lee, M. R. Leyden, Y. Kato and Y. Qi, *Chem. Mater.*, 2015, **27**, 1597-1603.
24. S. Pathak, A. Sepe, A. Sadhanala, F. Deschler, A. Haghighirad, N. Sakai, K. C. Goedel, S. D. Stranks, N. Noel, M. Price, S. Huettner, N. A. Hawkins, R. H. Friend, U. Steiner and H. J. Snaith, *ACS nano*, 2015, **9**, 2311-2320.
25. H. Gao, C. Ban, F. Li, T. Yu, J. Yang, W. Zhu, X. Zhou, G. Fu and Z. Zou, ACS Appl. Mater. Interfaces, 2015, **7**, 9110-9117.
26. J. H. Heo, D. H. Song, H. J. Han, S. Y. Kim, J. H. Kim, D. Kim, H. W. Shin, T. K. Ahn, C. Wolf, T. W. Lee and S. H. Im, *Adv. Mater.*, 2015, **27**, 3424-3430.
27. J. H. Heo, H. J. Han, D. Kim, T. K. Ahn and S. H. Im, *Energy Environ. Sci.*, 2015, **8**, 1602-1608.
28. F. X. Xie, D. Zhang, H. Su, X. Ren, K. S. Wong, M. Graetzel and W. C. H. Choy, *ACS nano*, 2015, **9**, 639-646.
29. J. You, Z. Hong, Y. M. Yang, Q. Chen, M. Cai, T. B. Song, C. C. Chen, S. Lu, Y. Liu, H. Zhou and Y. Yang, 2014, **8**, 1674-1680.

30. Y. Xiao, G. Han, Y. Li, M. Li and J. Wu, *J. Mater. Chem. A*, 2014, **2**, 16856-16862.
31. Y. Tidhar, E. Edri, H. Weissman, D. Zohar, G. Hodes, D. Cahen, B. Rybtchinski and S. Kirmayer, *J. Am. Chem. Soc.*, 2014, **136**, 13249-13256.
32. G. E. Eperon, V. M. Burlakov, P. Docampo, A. Goriely and H. J. Snaith, Adv. Funct. Mater., 2014, **24**, 151-157.

The table of contents entry:

The higher film coverage and better device performance is achieved for film spin-coated in air and then annealed in vacuum.